Vascular Pharmacology 151 (2023) 107194

Contents lists available at ScienceDirect

Vascular Pharmacology

journal homepage: www.elsevier.com/locate/vph

Prostacyclin mimetics inhibit DRP1-mediated pro-proliferative mitochondrial fragmentation in pulmonary arterial hypertension

Jeries Abu-Hanna [a,b], Evangelos Anastasakis [a,b], Jigisha A. Patel [a], Mohammad Mahmoud Rajab Eddama [d], Christopher P. Denton [b], Jan-Willem Taanman [c], David Abraham [b,1], Lucie H. Clapp [a,*,1]

[a] Centre for Cardiovascular Physiology and Pharmacology, Institute of Cardiovascular Science, University College London, London, United Kingdom
[b] Centre for Rheumatology, Division of Medicine, University College London, London, United Kingdom
[c] Department of Clinical and Movement Neurosciences, Queen Square Institute of Neurology, University College London, London, United Kingdom
[d] Department of Surgical Biotechnology, Division of Surgery and Interventional Science, University College London, London, United Kingdom

ARTICLE INFO

Keywords:
Prostacyclin
Dynamin-related protein 1
Mitochondria
Pulmonary arterial hypertension
Pulmonary arterial smooth muscle cells

ABSTRACT

Pulmonary arterial hypertension (PAH) is a rare cardiopulmonary disorder, involving the remodelling of the small pulmonary arteries. Underlying this remodelling is the hyper-proliferation of pulmonary arterial smooth muscle cells within the medial layers of these arteries and their encroachment on the lumen. Previous studies have demonstrated an association between excessive mitochondrial fragmentation, a consequence of increased expression and post-translational activation of the mitochondrial fission protein dynamin-related protein 1 (DRP1), and pathological proliferation in PASMCs derived from PAH patients. However, the impact of prostacyclin mimetics, widely used in the treatment of PAH, on this pathological mitochondrial fragmentation remains unexplored. We hypothesise that these agents, which are known to attenuate the proliferative phenotype of PAH PASMCs, do so in part by inhibiting mitochondrial fragmentation. In this study, we confirmed the previously reported increase in DRP1-mediated mitochondrial hyper-fragmentation in PAH PASMCs. We then showed that the prostacyclin mimetic treprostinil signals via either the Gs-coupled IP or EP_2 receptor to inhibit mitochondrial fragmentation and the associated hyper-proliferation in a manner analogous to the DRP1 inhibitor Mdivi-1. We also showed that treprostinil recruits either the IP or EP_2 receptor to activate PKA and induce the phosphorylation of DRP1 at the inhibitory residue S637 and inhibit that at the stimulatory residue S616, both of which are suggestive of reduced DRP1 fission activity. Like treprostinil, MRE-269, an IP receptor agonist, and butaprost, an EP_2 receptor agonist, attenuated DRP1-mediated mitochondrial fragmentation through PKA. We conclude that prostacyclin mimetics produce their anti-proliferative effects on PAH PASMCs in part by inhibiting DRP1-mediated mitochondrial fragmentation.

1. Introduction

Pulmonary arterial hypertension (PAH) is a rare, progressive, and frequently fatal cardiopulmonary disorder, characterised by occlusive remodelling of the small pulmonary arteries [1–3]. Pulmonary arterial luminal obliteration in PAH leads to a rise in pulmonary vascular resistance and pulmonary arterial pressure [1,2]. The resultant increase in right heart afterload causes right ventricular hypertrophy and ultimately death from right ventricular failure [1,2,4]. Central to pulmonary vascular remodelling is the heightened proliferation and apoptosis-resistance of pulmonary arterial smooth muscle cells (PASMCs), a neoplastic phenotype that persists in cell culture [5–7]. The proposed metabolic theory of PAH posits that the pathological hyper-proliferation of PASMCs is associated with reprogramming of cellular energetics, namely a Warburgian shift from mitochondrial oxidative phosphorylation to cytosolic glycolysis as well as excessive mitochondrial fragmentation linked to heightened G2-to-M transition of the cell cycle [7–10].

* Corresponding author at: Centre for Cardiovascular Physiology and Pharmacology, Institute of Cardiovascular Science, University College London, London, United Kingdom.
E-mail address: l.clapp@ucl.ac.uk (L.H. Clapp).
[1] Joint senior authors

https://doi.org/10.1016/j.vph.2023.107194
Received 25 April 2023; Received in revised form 23 June 2023; Accepted 10 July 2023
Available online 11 July 2023

Mitochondria form highly dynamic networks that continuously undergo cycles of fusion and fission [11–13]. Mitochondrial fusion is mediated by the mitochondrial membrane-anchored GTPases mitofusin-1 (MFN1), MFN2 and optic atrophy-1 (OPA1) [11–13]. Mitochondrial fission, on the other hand, is mediated by the cytosolic GTPase dynamin-related protein 1 (DRP1) [11–13]. In the cytosol, DRP1 exists in an inactive state and, upon activation, translocates to fission sites at the outer mitochondrial membrane (OMM), where it interacts with one or more of its membrane-anchored binding partners. DRP1 binding proteins include fission protein 1 (FIS1), mitochondrial fission factor (MFF) and mitochondrial dynamics proteins of 49 and 51 kDa (MiD49 and MiD51) [11–13]. Following recruitment to the OMM, DRP1 multimerises into ring structures, which constrict and ultimately sever the mitochondria. DRP1 activity is predominantly regulated by post-translational phosphorylation of two serine (S) residues within its GTPase effector domain [11–13]. Phosphorylation of S616 stimulates DRP1 activity and is mediated by a number of serine-threonine kinases, including cyclin B1/cyclin-dependent kinase 1 (CDK1) and extracellular signal regulated kinase 2 (ERK2) [14,15]. Phosphorylation of S637 inhibits DRP1 GTPase activity and is exclusively catalysed by cyclic adenosine monophosphate (cAMP)-dependent protein kinase A (PKA) downstream of Gs-coupled receptors, whereas S637 dephosphorylation is mediated by the phosphatase calcineurin and serves to activate DRP1 [16–19].

In PAH, PASMC hyperproliferation has been associated with increased mitochondrial fission due to heightened expression and activating phosphorylation of DRP1 at S616 [20]. DRP1 hyperphosphorylation was attributed to increased activity of the cell cycle regulator CDK1 and its activator cyclin B1 and associated with enhanced G2 to mitosis transition of the cell cycle [20]. Increased mitochondrial fission in PAH PASMCs has also been shown to occur as consequence of increased expression of FIS1, MiD49 and MiD51, enhancing the recruitment of DRP1 to mitochondrial fission sites [20,21].

To date, the impact of existing PAH therapies on the impaired mitochondrial dynamics in PAH remains unexplored. Prostacyclin and its mimetics constitute the gold standard treatment for patients with severe PAH, delaying disease progression and improving survival [22,23]. These agents have been shown to exert strong vasodilatory effects on the pulmonary vasculature, as well as anti-proliferative effects on PASMCs, derived from both normal and PAH lungs [24–30]. Prostacyclin mimetics were originally thought to signal solely via the prostanoid IP receptor to produce these effects. However, recent evidence suggests that prostacyclin mimetics activate other prostanoid receptor subtypes [31]. Treprostinil, for example, was found to inhibit normal PASMC proliferation predominantly via the IP prostanoid receptor while also recruiting the EP_2 receptor to inhibit the proliferation of PAH PASMCs [26,27]. The shift from IP to EP_2 receptor signaling by treprostinil in PAH PASMCs is believed to be a consequence of IP receptor downregulation coupled with EP_2 receptor upregulation [26,27].

In the present study, we investigated mitochondrial network morphology and the expression of proteins of the mitochondrial fusion and fission machinery in PAH PASMCs. We sought to determine whether the prostacyclin analogue treprostinil inhibits PASMC proliferation by attenuating the enhanced mitochondrial fission previously reported in PAH PASMCs. We also sought to delineate which prostanoid receptors and downstream signaling proteins were involved in mediating any modulatory effects observed.

2. Materials and methods

2.1. Cell culture

Control PASMCs were obtained from the resected lungs of patients with suspected malignancy ($n = 3$) derived from sites distant from the tumour. PAH PASMCs ($n = 6$) were derived from the lungs of patients with end-stage idiopathic PAH after having died or undergone transplant (Supplementary Table 1). Ethical approval was obtained from Research Ethics Committees at the Great Ormond Street Hospital (ICH and GOSH REC 05/Q0508/45) and the Assistance Public-Hopitaux de Paris (IRB00006477, agreement No. 11–0450). Control or PAH PASMCs were cultured in Dulbecco's modified Eagle's medium/nutrient mix (DMEM/F12; Gibco), supplemented with 10% (v/v) foetal bovine serum (FBS) and 1% (v/v) penicillin/streptomycin (Gibco), in a humidified atmosphere of 5% CO_2 at 37 °C. Only PASMCs between passages 2 and 10 were used in the experiments.

2.2. Cell proliferation

PASMCs were seeded in 6-well plates at a density of 20,000 cells/ml and maintained in 10% FBS for 24 h. PASMCs were then starved in 0.1% FBS for 48 h to induce growth arrest. After serum-starvation, PASMCs were treated as indicated in the results in DMEM/F12 with 10% FBS for 96 h, trypsinised and counted using 0.4% trypan blue stain (Invitrogen) and Neubauer improved C-Chip disposable haemocytometers (NanoEnTek).

2.3. Immunoblotting

PASMCs grown in monolayers were lysed in radioimmunoprecipitation assay (RIPA) buffer supplemented with cOmplete™ protease inhibitor (Roche) and phosphatase inhibitor cocktails 2 and 3 (Sigma-Aldrich). Lysates were centrifuged at 1000 x*g* at 4 °C for 10 min and resultant supernatants were stored at −80 °C until used. Protein concentrations were determined using the Pierce BCA Assay Kit (ThermoFisher Scientific). Equal amounts of proteins (10–25 μg) were resolved on NuPAGE™ 4–12% Bis-Tris Gels (Invitrogen) alongside SeeBlue Plus2 pre-stained protein standard (Invitrogen) and then transferred to Amersham Protran nitrocellulose membranes (GE Healthcare). Membranes were blocked in Tris-buffered saline containing 0.1% (*v*/v) Tween-20 (TBST) and 5% (*w/v*) skimmed milk before being incubated overnight at 4 °C with primary antibodies, diluted in TBST with 5% (w/v) bovine serum albumin (BSA), against DRP1 (1:1000, Cell Signaling Technology), pDRP1 S616 (1:1000; Cell Signaling Technology), pDRP1 S637 (1:1000; Abcam), MFN1 (1:1000; Abcam), MFN2 (1:1000; Abcam), OPA1 (1:1000; R&D Systems) and GAPDH (1:50,000; Abcam). Membranes were then incubated with the appropriate HRP-linked secondary antibody, either anti-mouse (1:1000; Cell Signaling Technology) or anti-rabbit (1:1000; Cell Signaling Technology), for 1 h at room temperature. Bands were detected using Amersham ECL Western Blotting Detection Reagents (GE Healthcare) with exposure to sheets of Amersham Hyperfilm ECL (GE Healthcare). Densitometry was performed using ImageJ.

2.4. Immunohistochemistry

Control or PAH lung tissues were formalin-fixed and paraffin-embedded (FFPE). FFPE sections (3 μm in thickness) were deparaffinised in xylene followed by gradual rehydration in 100–75% (*v*/v) ethanol and ultimately water. Heat-induced antigen retrieval was performed at pH 6 using 10 mM sodium citrate buffer with 0.05% (v/v) Tween® 20 (Sigma-Aldrich) for 20 min in a microwave set to full power. Following antigen retrieval, sections were stained for DRP1 using the Novolink Polymer Detection System (Leica Biosystems) according to the manufacturer's instructions. Endogenous peroxidases were first neutralised by incubating the sections with Peroxidase Block for 5 min at room temperature. Sections were then treated with Novacastra Protein Block for 15 min followed by incubation with the primary rabbit antibody against DRP1 (1:250; Novus Biologicals) or normal rabbit IgG (Cell Signaling Technology) diluted in Antibody diluent (Dako) for 1 h at room temperature. Sections were then incubated with the Novolink Polymer for 30 min before being developed with DAB working reagent, composed of 1 part Novocastra DAB chromogen and 20 parts Novolink

DAB Substrate Buffer, for 5 min. Sections were counterstained with Meyer's hemotoxylin and dehydrated by passing them through increasing concentrations of ethanol (75–100% (*v*/v)) and xylene. Sections were mounted with DPX Mounting Medium (ThermoFisher Scientific). Images were acquired using the Nanozoomer S360 Digital slide scanner (Hamamatsu) and viewed on NDP.view 2 (Hamamatsu).

2.5. Live cell assessment of mitochondrial network morphology

PASMCs were seeded at a density of 10,000 cells/ml in glass-bottom μ-dishes (Ibidi), maintained in DMEM/F12 with 10% FBS for 48 h and serum-starved in DMEM/F12 with 0.1% FBS for 48 h. After serum starvation, cells were incubated with 10 μg/ml Hoechst 33342 (nuclear dye; Invitrogen) and 25 nM tetramethylrhodamine methyl ester (TMRM; mitochondrial dye; Invitrogen) in Hank's balanced salt solution (HBSS) with 10 mM HEPES (StemCell Technologies) for 30 min and imaged with Nikon Eclipse Ti-E inverted microscope equipped with a 60× oil objective. The Mitochondrial Network Analysis (MiNA) toolset developed by Valente et al. [32] was used to perform mitochondrial morphometry on ImageJ (NIH). This freely available ImageJ macro enhances the quality of images prior to binarization and skeletonization to enable the quantification of various aspects of mitochondrial network morphology, including mitochondrial branch length, number of branches per mitochondrial network, number of mitochondrial networks, number of individual mitochondria and mitochondrial footprint. The MINA toolset identifies individual mitochondria as punctate, rod and large, round structures, and mitochondrial networks as structures with at least one central node and three branches.

2.6. Statistical analysis

Statistical analyses were performed using GraphPad Prism 8. In the results, values are shown as means ± standard error of the mean (SEM) and *n* denotes the number of different control or PAH patients. SEM allows inferences about the patient population to be made from our sample of patients. Unpaired Student's *t*-test was used to compare the means of two unrelated groups. One-way analysis of variance (ANOVA) with Bonferroni's post hoc test for multiple comparisons was used to compare the means of three or more independent groups. Two-way ANOVA with Sidak's post hoc test for multiple comparisons was used to compare the mean differences between groups that have been split on two independent variables (e.g., treatment and time). Paired student's *t*-test or repeated measures one-way ANOVA with Tukey's post hoc test were used where groups were normalised to a control group. Only significant *p* values (i.e. $p < 0.05$) were indicated on the figures.

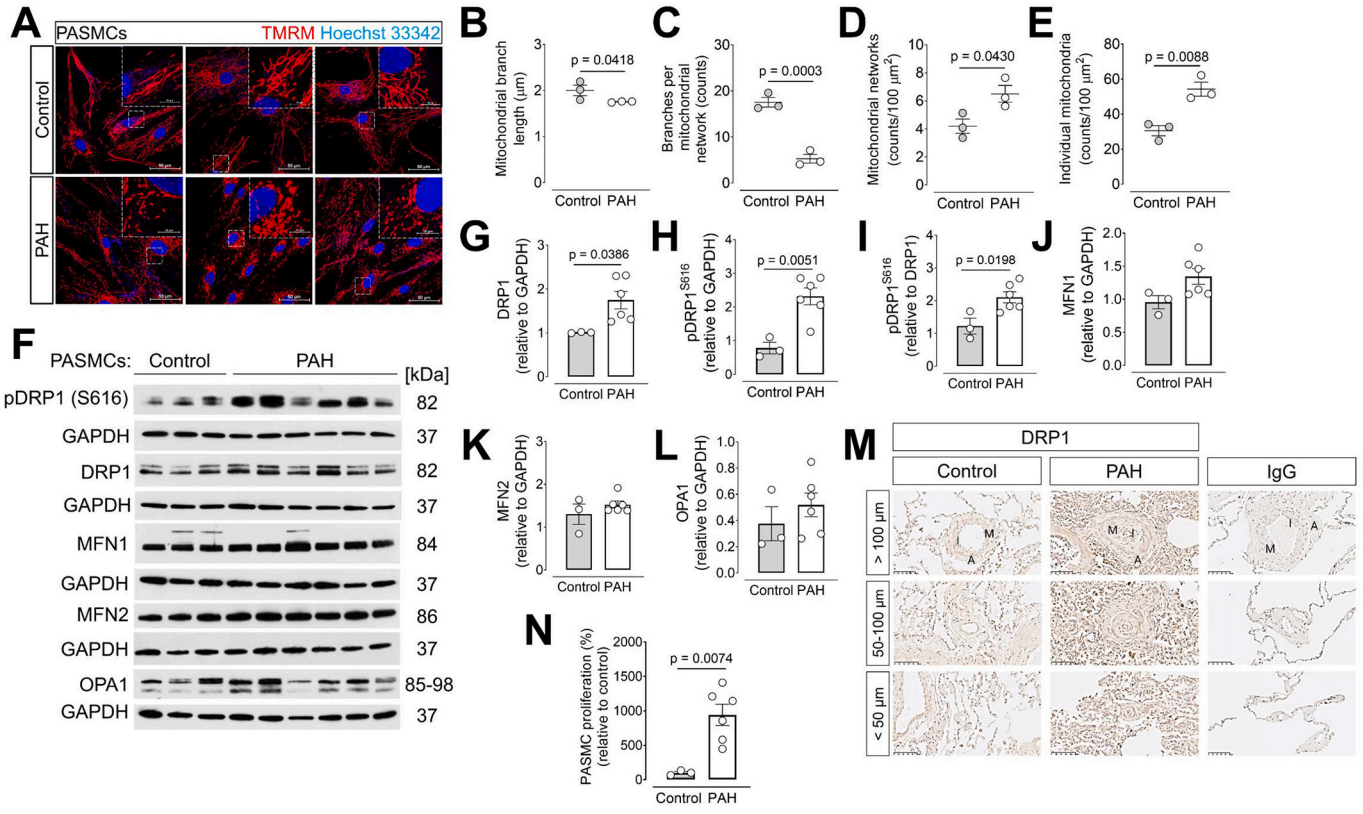

Fig. 1. Enhanced mitochondrial fission in hyperproliferative PAH PASMCs is a consequence of increased expression and stimulatory phosphorylation of DRP1 at S616. (A) Serum-starved control ($n = 3$) and PAH ($n = 3$) PASMCs were stained with Hoechst 33342 (nuclei; blue) and TMRM (mitochondria; red) and imaged by confocal microscopy. Scale bars: 10 and 50 μm. (B) Mitochondrial branch length, (C) number of branches per mitochondrial network, (D) number of mitochondrial networks and (E) number of individual mitochondria were determined by mitochondrial morphometry. (F) Immunoblotting of proteins from serum-starved control ($n = 3$) and PAH ($n = 6$) PASMCs for DRP1 and its activated form pDRP1^{S616}, as well as MFN1, MFN2 and OPA1. GAPDH served as a loading control. Protein expression of (G) DRP1, (H) pDRP1^{S616}, (J) MFN1, (K) MFN2 and (L) OPA1 relative to GAPDH. (I) pDRP1^{S616} expressed as a ratio of total DRP1 in control and PAH PASMCs. (M) Immunohistochemical staining of control and PAH lung sections for DRP1 with arteries stratified according to their diameters as indicated and the intimal (I), medial (M) and adventitial (A) layers annotated. Staining with normal IgG to confirm specificity of the DRP1 staining. Scale bar: 100 μm. (N) Proliferation of control ($n = 3$) and PAH ($n = 6$) PASMCs in response to 10% FBS for 96 h. Values are means ± SEM. Unpaired Student's *t*-test in B, C, D, E, G, H, J, K, and L, and paired Student's *t*-test was used in N. (For interpretation of the references to colour in this figure legend, the reader is referred to the web version of this article.)

3. Results

3.1. Increased expression and stimulatory phosphorylation of DRP1 underlie excessive mitochondrial fission in hyperproliferative PAH PASMCs

We first assessed mitochondrial morphology in control and PAH PASMCs to confirm the previously reported increase in mitochondrial fragmentation in PAH PASMCs [20]. Cultured control and PAH PASMCs were stained with the mitochondrial dye TMRM and the nuclear dye Hoechst 33342 followed by confocal imaging (Fig. 1A). The MiNA toolset on ImageJ was used to analyse mitochondrial network morphology. Mitochondrial branches were significantly longer (Fig. 1B) and more numerous (Fig. 1C) in control PASMCs, compared to PAH

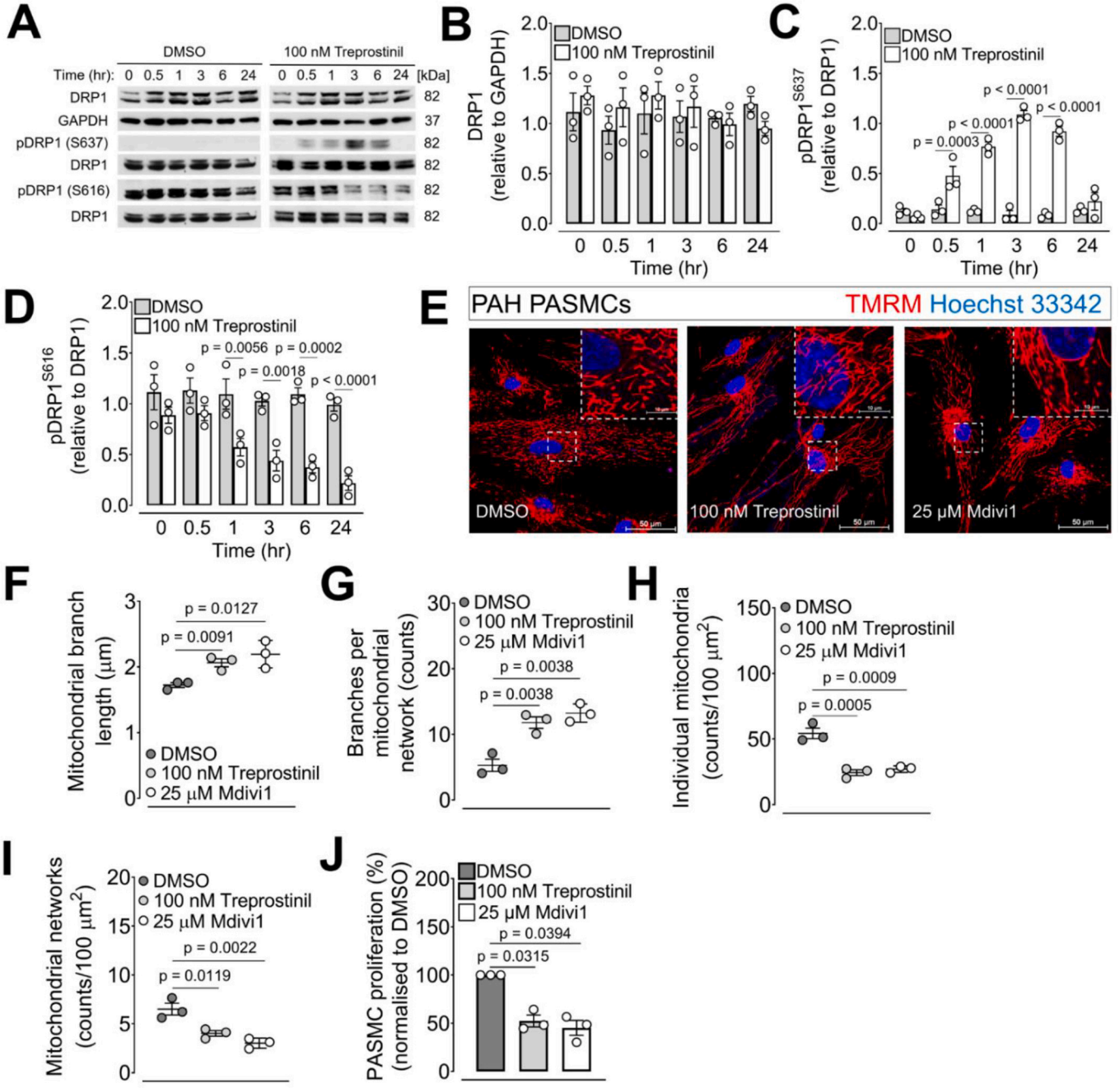

Fig. 2. Treprostinil influences post-translational phosphorylation of DRP1 to attenuate mitochondrial fission and proliferation in PAH PASMCs. (A) Proteins from serum-starved PAH PASMCs ($n = 3$) treated with either DMSO or 100 nM treprostinil for the indicated times were immunoblotted for total DRP1, pDRP1^{S637} and pDRP1^{S616}. Protein levels of (B) total DRP1 relative to GAPDH and (C) pDRP1^{S637} or (D) pDRP1^{S616} relative to total DRP1 were determined by densitometry. (E) Serum-starved PAH ($n = 3$) PASMCs were treated with either DMSO, 100 nM treprostinil or 25 μM Mdivi1 for 3 h, stained with Hoechst 33342 (nuclei; blue) and TMRM (mitochondria; red) and imaged by confocal microscopy. Scale bar: 50 μm. (F) Mitochondrial branch length, (G) number of branches per mitochondrial network, (H) number of individual mitochondria number of mitochondrial networks and (I) number of mitochondrial networks were determined by mitochondrial morphometry. (J) Proliferation of PAH PASMCs ($n = 3$) in response to 10% FBS for 96 h in the presence of DMSO, 100 nM treprostinil or 25 μM Mdivi1. Values are means ± SEM. Two-way ANOVA with Sidak's test for multiple comparisons was used in B, C and D. One-way ANOVA with Bonferroni's test for multiple comparisons was used in F, G, H and I. Repeated measures one-way ANOVA with Tukey's test for multiple comparisons was used in J. (For interpretation of the references to colour in this figure legend, the reader is referred to the web version of this article.)

PASMCs. Moreover, PAH PASMCs contained higher numbers of mitochondrial networks (Fig. 1D) and individual mitochondria mitochondrial networks (Fig. 1E) per 100 μm^2 mitochondrial footprint, particularly in perinuclear regions, than control PASMCs. Collectively, these findings suggest that mitochondrial fragmentation is increased in PAH PASMCs.

Given the augmented mitochondrial fission in PAH PASMCs, we assessed the expression and activating phosphorylation of DRP1, as well as the expression of MFN1, MFN2 and OPA1 in PAH PASMCs compared to control PASMCs. Immunoblotting (Fig. 1F) revealed significantly higher protein expression of total DRP1 (Fig. 1G) and DRP1 phosphorylated at S616 (Fig. 1H) relative to GAPDH in cultured PAH PASMCs than in their control counterparts. Moreover, the ratio of DRP1 phosphorylated at S616 to total DRP1 (Fig. 1I) was markedly higher in PAH PASMCs than in control PASMCs, suggesting that increased DRP1 protein expression is accompanied by increased stimulatory phosphorylation at S616. Expression of the mitochondrial fusion proteins MFN1 (Fig. 1J), MFN2 (Fig. 1K) and OPA1 (Fig. 1L) appeared to be unaltered in PAH PASMCs, suggesting that the mitochondrial fusion machinery remains intact.

After confirming upregulation of DRP1 in cultured PAH PASMCs, immunohistochemical staining of lung sections from control and PAH patients was performed to assess DRP1 protein expression in situ within the medial layers of distal pulmonary arteries (diameter < 200 μm), the primary sites of disease pathology (Fig. 1M). In contrast to the control lung sections, the medial layers of the remodelled pulmonary arteries in the PAH lung sections stained more strongly for DRP1, corroborating the increased DRP1 expression observed in cultured PAH PASMCs. Proliferation of PAH PASMCs in response to 10% FBS was significantly higher than that of control PASMCs (Fig. 1N), confirming their pathologically hyperproliferative phenotype. Taken together, these results suggest that a tip in the balance between mitochondrial fusion and fission in favour of fission in PAH PASMCs leads to hyperproliferation.

3.2. Treprostinil alters post-translation phosphorylation of DRP1 to inhibit mitochondrial fission in PAH PASMCs

To explore the effect of treprostinil on DRP1 expression and post-translational phosphorylation, PAH PASMCs were treated with either DMSO (control) or treprostinil for 0, 0.5, 1, 3, 6 and 24 h and proteins were extracted and immunoblotted for total DRP1, DRP1 phosphorylated at the inhibitory residue S637 and DRP1 phosphorylated at the activating residue S616 (Fig. 2A). Treprostinil had no effect on the expression of total DRP1 relative to GAPDH at any of the time points (Fig. 2B). Treprostinil did, however, stimulate DRP1 phosphorylation at the inhibitory site S637 (Fig. 2C) and inhibit DRP1 phosphorylation at the stimulatory site S616 (Fig. 2D). DRP1 phosphorylation at S637 was observed 0.5 h after treatment with treprostinil with maximal phosphorylation occurring 3 h after treatment. Treprostinil-induced DRP1 phosphorylation at S637 lasted for 6 h but subsided 24 h after treatment, underpinning the transiency of this inhibitory phosphorylation event. Inhibition of DRP1 phosphorylation at S616 was observed 1 h after treatment with 100 nM treprostinil and persisted for 24 h. Taken together, these results indicate that treprostinil inhibits the activity of the mitochondrial fission protein DRP1 by influencing its post-translational phosphorylation rather than its expression.

Given the inhibitory effect of treprostinil on DRP1 activity, we assessed the effect of treprostinil on mitochondrial fragmentation in PAH PASMCs and compared it with that of the DRP1 small-molecule inhibitor Mdivi1. Treating PAH PASMCs with treprostinil or Mdivi1 for 3 h similarly increased the number of branches per mitochondrial network (Fig. 2G) as well as the length of these branches (Fig. 2F), while reducing the numbers of individual mitochondria (Fig. 2H) and mitochondrial networks (Fig. 2I) per 100 μm^2 mitochondrial footprint. The fusogenic effects of treprostinil and Mdivi1 on the mitochondria were associated with comparable inhibitory effects on the proliferation of PAH PASMCs (Fig. 2J). Collectively, these results suggest that, in PAH PASMCs, treprostinil inhibits the mitochondrial fission protein DRP1 to promote the formation of fewer, larger, highly branched mitochondrial networks and reduce proliferation in a manner similar to the DRP1 inhibitor Mdivi1.

3.3. Treprostinil signals via either the IP or EP$_2$ receptor to activate PKA and inhibit DRP1 activity in PAH PASMCs

We next sought to identify the membrane receptors through which treprostinil signals to alter the phosphorylation of DRP1 and promote mitochondrial elongation. Treprostinil has been shown to activate the IP and EP$_2$ prostanoid receptors in PAH PASMCs [26,27]. We therefore used the antagonists RO1138452 and PF04418948 to block the IP and EP$_2$ receptors, respectively [27]. Individually, RO1138452 and PF04418948 had no effect on the treprostinil-induced phosphorylation of DRP1 at S637 (Fig. 3A and B) or the treprostinil-mediated inhibition of DRP1 phosphorylation at S616 (Fig. 3A and C). Moreover, live-cell imaging (Fig. 3D) revealed that, individually, RO1138452 and PF04418948 had no effect on the treprostinil-stimulated increase in mitochondrial branch length (Fig. 3E) and branches per mitochondrial network (Fig. 3F) or the treprostinil-induced decrease in individual mitochondria (Fig. 3G) and mitochondrial networks per 100 μm^2 mitochondrial footprint (Fig. 3H). However, in combination, RO1138452 and PF04418948 completely blocked the treprostinil-induced DRP1 phosphorylation at S637 (Fig. 3B) and the treprostinil-mediated inhibition of DRP1 phosphorylation at S616 (Fig. 3C). Together, these two antagonists also reversed the treprostinil-stimulated increase in mitochondrial branch length and branches per mitochondrial network and the treprostinil-induced decrease in the numbers of individual mitochondria and mitochondrial networks per 100 μm^2 mitochondrial footprint (Fig. 3D-H). The fusogenic effect of treprostinil was accompanied by a 40% decrease in PAH PASMC proliferation, which was abrogated by the antagonists RO1138452 and PF04418948 when administered together (Fig. 3I) These results suggest that, in PAH PASMCs, treprostinil recruits either the IP or EP$_2$ receptor to inhibit DRP1, promote mitochondrial elongation and inhibit proliferation.

The IP and EP$_2$ receptors couple via Gs to elevate cAMP and activate PKA. To determine whether PKA is required for the effect of treprostinil on DRP1 phosphorylation, the PKA inhibitor H89 was used. H89 blocked treprostinil-induced DRP1 phosphorylation at S637 as well as treprostinil-mediated inhibition of DRP1 phosphorylation at S616, highlighting the requirement of PKA for the effect of treprostinil on DRP1 phosphorylation (Fig. 3A-C). Moreover, H89 blocked the treprostinil-induced decrease in the numbers of individual mitochondria and mitochondrial networks per 100 μm^2 mitochondrial footprint and the treprostinil-induced increase in mitochondrial branch length and branches per mitochondrial network (Fig. 3D-H). The antiproliferative effect of treprostinil on PAH PASMCs was blocked by H89 (Fig. 3I).

3.4. IP or EP$_2$ receptor agonism attenuates mitochondrial fission and proliferation in PAH PASMCs

To confirm the ability of the IP and EP$_2$ receptors to inhibit DRP1 activity and attenuate mitochondrial fission in PAH PASMCs, the IP receptor agonist MRE-269 and the EP$_2$ receptor agonist butaprost were utilised to activate the IP and EP$_2$ receptor individually. MRE-269 (Fig. 4A-C) and butaprost (Fig. 5A-C) both stimulated inhibitory DRP1 phosphorylation at S637 and inhibited activating DRP1 phosphorylation at S616 in PAH PASMCs. The effect of MRE-269 on DRP1 phosphorylation at both serine residues was blocked by the IP receptor antagonist RO1138452, confirming its selectivity for the IP receptor, and by the PKA inhibitor H89, highlighting the requirement of PKA downstream of the IP receptor (Fig. 4A-C). The effect of butaprost on DRP1 phosphorylation at both serine residues was blocked by the EP$_2$ receptor antagonist PF04418948, underpinning butaprost's preference for activating

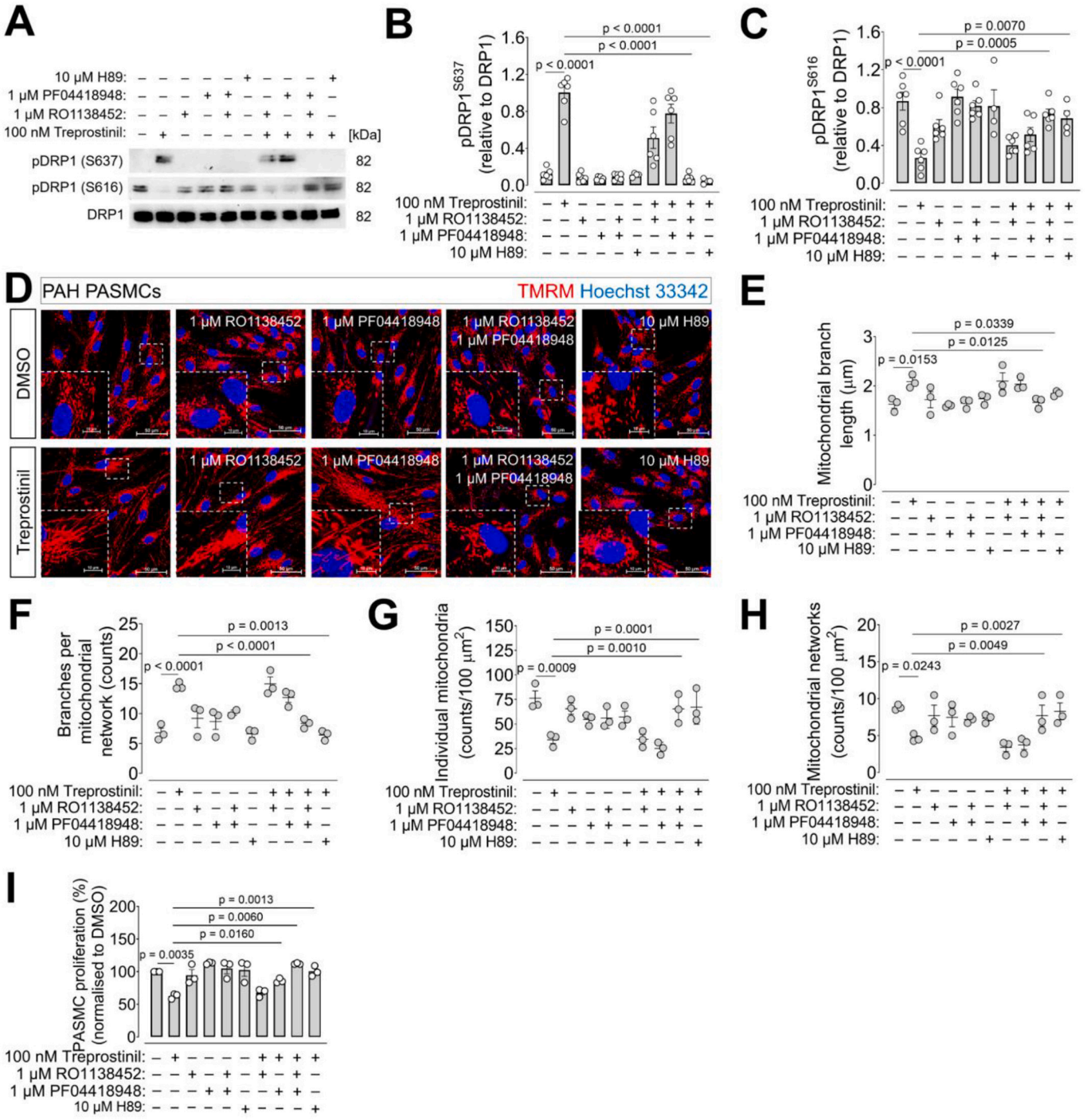

Fig. 3. Treprostinil signals via either the IP or EP_2 receptor to activate PKA and inhibit DRP1 and mitochondrial fission in PAH PASMCs. (A) Proteins from PAH PAMSCs ($n = 4$–6) pre-treated with DMSO, 1 μM RO1138452, 1 μM PF04418948, a combination of 1 μM RO1138452 and 1 μM PF04418948 or 10 μM H89 for 30 min and stimulated with DMSO or 100 nM treprostinil for 3 h were immunoblotted for total DRP1, $pDRP1^{S637}$ and $pDRP1^{S616}$. Protein levels of (B) $pDRP1^{S637}$ and (C) $pDRP1^{S616}$ relative to total DRP1 were determined by densitometry. (D) Serum-starved PAH PASMCs ($n = 3$) pre-treated with the indicated antagonists for 30 min and stimulated with either DMSO or 100 nM treprostinil for 3 h were stained with Hoechst 33342 (nuclei; blue) and TMRM (mitochondria; red) and imaged by confocal microscopy. Scale bars: 50 and 100 μm. (E) Mitochondrial branch length, (F) number of branches per mitochondrial network, (G) number of individual mitochondria and (H) number of mitochondrial networks were determined by mitochondrial morphometry. (I) Proliferation of PAH PASMCs ($n = 3$) pre-treated with the indicated antagonists for 30 min and subjected to DMSO or 100 nM treprostinil in 10% FBS for 96 h. Values are means ± SEM. One-way ANOVA with Bonferroni's test for multiple comparisons was used in B, C, E, F, G, and H. Repeated measures one-way ANOVA with Tukey's test for multiple comparisons was used in I. (For interpretation of the references to colour in this figure legend, the reader is referred to the web version of this article.)

the EP_2 receptor, and by H89, implicating PKA downstream of the EP_2 receptor (Fig. 5A-C).

Fluorescence staining of PAH PASMCs (Fig. 4D and Fig. 5D) revealed that, like treprostinil, MRE-269 (Fig. 4E and F) and butaprost (Fig. 5E and F) increased the number of branches per mitochondrial network and the length of these branches. MRE-269 (Fig. 4G and H) and butaprost (Fig. 5G and H) also considerably reduced the numbers of individual mitochondria and mitochondrial networks per 100 $μm^2$ mitochondrial

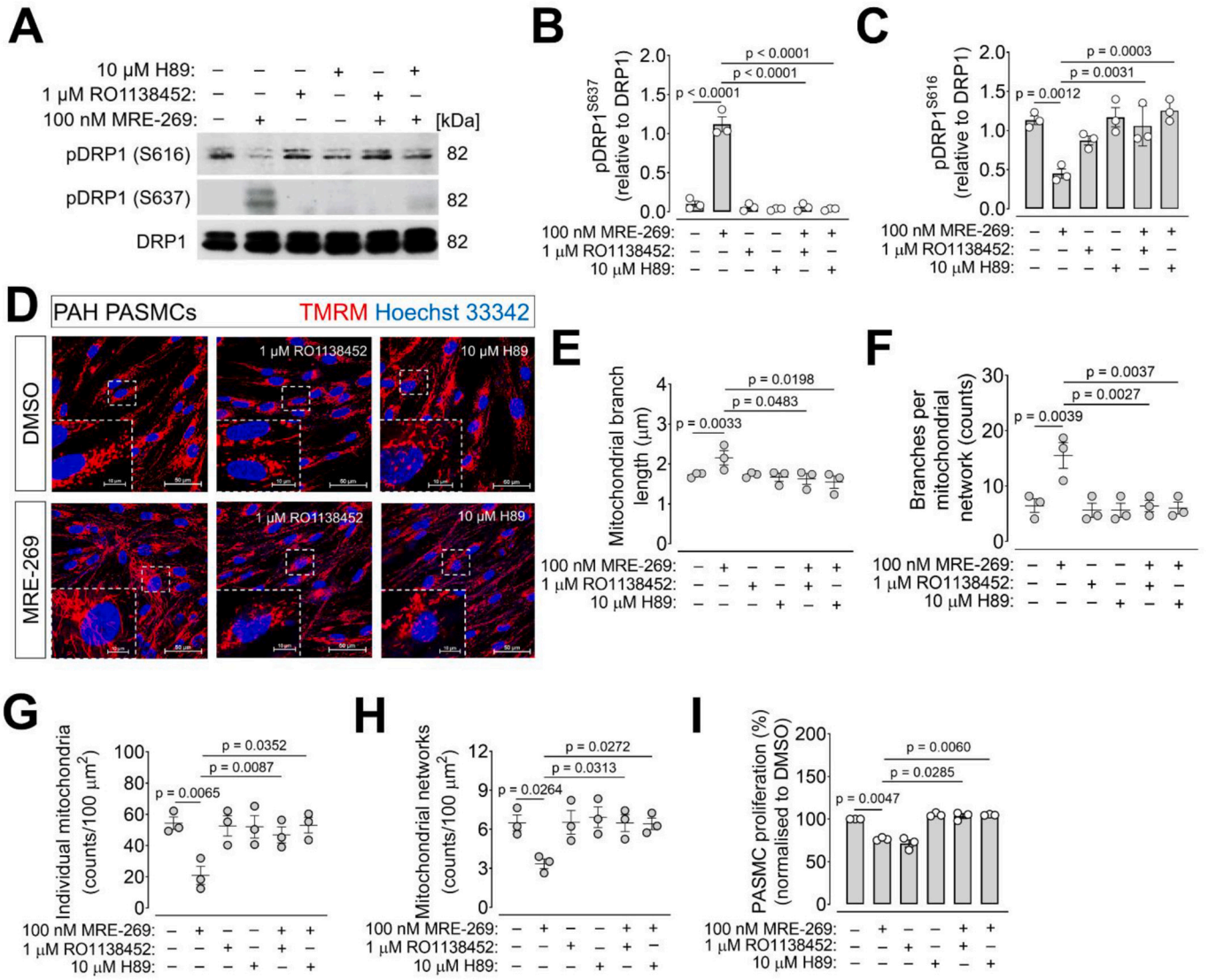

Fig. 4. Individual IP receptor agonism inhibits DRP1 to attenuate mitochondrial fission and proliferation in PAH PASMCs. (A) Proteins from serum-starved PAH PASMCs ($n = 3$) pre-treated with DMSO, 1 μM RO1138452 or 10 μM H89 for 30 min and stimulated with DMSO or 100 nM MRE-269 for 3 h were immunoblotted for total DRP1, pDRP1^{S637} and pDRP1^{S616}. Protein levels of (B) pDRP1^{S637} and (C) pDRP1^{S616} relative to total DRP1 were determined by densitometry. (D) Serum-starved PAH PASMCs ($n = 3$) pre-treated with the indicated antagonists and stimulated with either DMSO or MRE-269 were stained with Hoechst 33342 (nuclei; blue) and TMRM (mitochondria; red) and imaged by confocal microscopy. Scale bar: 10 and 50 μm. (E) Mitochondrial branch length, (F) number of branches per mitochondrial network, (G) number of individual mitochondria and (H) number of mitochondrial networks were determined by mitochondrial morphometry. (I) Proliferation of PAH PASMCs ($n = 3$) pre-treated with the indicated antagonists for 30 min and subjected to DMSO or 100 nM MRE-269 in 10% FBS for 96 h. Values are means ± SEM. One-way ANOVA followed by Bonferroni's test for multiple comparisons was used in B, C, E, F, G, and H. Repeated measures one-way ANOVA with Tukey's test for multiple comparisons was used in I. (For interpretation of the references to colour in this figure legend, the reader is referred to the web version of this article.)

footprint. The fusogenic effects of MRE-269 and butaprost were associated with anti-proliferative effects on PAH PASMCs, which were blocked by RO1138452 and PF04418948, respectively, and by H89 (Fig. 4I and 5I, respectively). These findings further support the ability of the IP and EP_2 receptors to signal via PKA to influence DRP1 post-translational phosphorylation and inhibit proliferation in PAH PASMCs.

4. Discussion

The rapid and transient morphological changes in mitochondrial networks are crucial for many cellular processes, including proliferation, apoptosis and mitophagy [12]. For example, mitochondrial fission has been shown to precede the M phase of the cell cycle and its abrogation arrests the cell cycle at the G2/M checkpoint [15,33]. Marsboom et al. [20] was the first to demonstrate that underlying the hyper-proliferative phenotype of PAH PASMCs are highly fragmented mitochondria produced as a result of a tip in the balance between the processes of mitochondrial fission and fusion in favour of fission. This study also revealed morphological changes in the mitochondria in PAH PASMCs akin to those observed by Marsboom et al. [20] PAH PASMCs were shown to contain greater numbers of individual mitochondria, which encompass punctate, rod and large, round mitochondrial structures, and mitochondrial networks or mitochondrial structures, with at least one central node and three branches, than control PASMCs. Moreover, mitochondrial branches appeared to be longer and more numerous in control PASMCs than in their PAH equivalents. Collectively, these results suggest that mitochondrial fission and fragmentation are increased in PAH PASMCs, resulting in the appearance of numerous small, weakly branched mitochondrial networks and individuals.

Mitochondrial fission is the process by which a mitochondrion

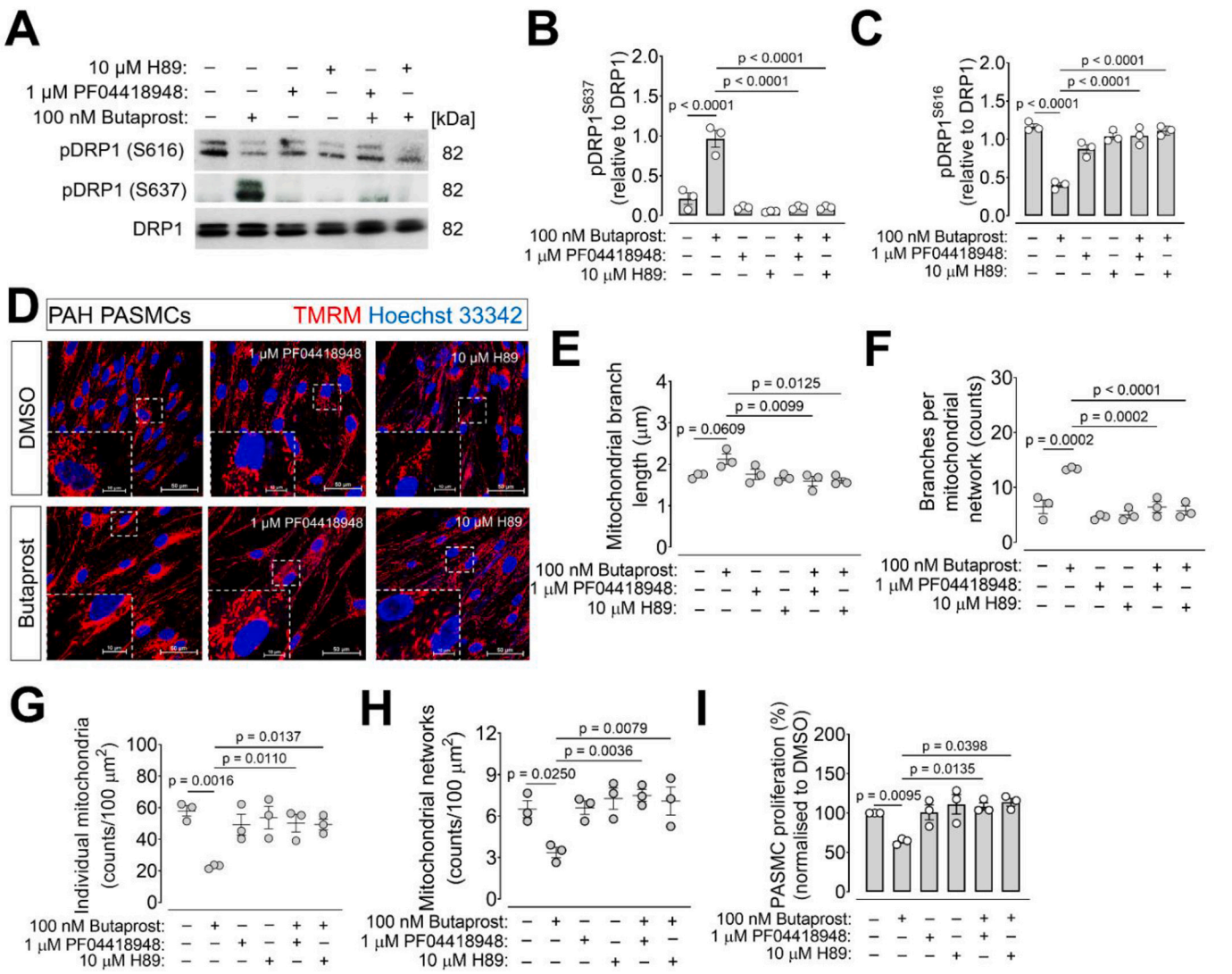

Fig. 5. Individual EP_2 receptor agonism inhibits DRP1 to attenuate mitochondrial fission and proliferation in PAH PASMCs. (A) Proteins from serum-starved PAH PASMCs ($n = 3$) pre-treated with DMSO, 1 μM PF04418948 or 10 μM H89 for 30 min and stimulated with DMSO or 100 nM butaprost were immunoblotted for total DRP1, $pDRP1^{S637}$ and $pDRP1^{S616}$. Protein levels of (B) $pDRP1^{S637}$ and (C) $pDRP1^{S616}$ relative to total DRP1 were determined by densitometry. (D) Serum-starved PAH PASMCs pre-treated with the indicated antagonists and stimulated with either DMSO or 100 nM butaprost were stained with Hoechst 33342 (nuclei; blue) and TMRM (mitochondria; red) and imaged by confocal microscopy. Scale bars: 50 and 100 μm. (E) Mitochondrial branch length, (F) number of branches per mitochondrial network, (G) number of individual mitochondria and (H) number of mitochondrial networks. (I) Proliferation of PAH PASMCs ($n = 3$) pre-treated with the indicated antagonists for 30 min and subjected to DMSO or 100 nM butaprost in 10% FBS for 96 h. Values are means ± SEM. One-way ANOVA with Bonferroni's test for multiple comparisons was used in B, C, E, F, G, and H. Repeated measures one-way ANOVA with Tukey's test for multiple comparisons was used in I. (For interpretation of the references to colour in this figure legend, the reader is referred to the web version of this article.)

divides into two smaller mitochondria. The primary mediator of mitochondrial fission is DRP1, a large monomeric GTPase [12]. DRP1 monomers are recruited from the cytosol to potential fission sites on the mitochondrial surface, where they assemble into ring or spiral structures that wrap around and constrict mitochondrial tubules [11]. Because of the increased mitochondrial fission observed in PAH PASMCs and the central role of DRP1 in mediating mitochondrial fission, it was posited that DRP1 expression and activity might also be elevated in PAH PASMCs. Indeed, protein expression of DRP1 was found to be considerably higher in cultured PAH PASMCs than in their control counterparts. Moreover, stronger DRP1 expression was observed in the medial layers of distal pulmonary arteries in PAH lung tissue sections than in those derived from control subjects. This is in agreement with the increased DRP1 expression in PAH PASMCs reported by Marsboom et al. [20] DRP1 activity is increased by phosphorylation at S616, which is mediated by a variety of serine/threonine kinases. For example, during the cell cycle, DRP1 is phosphorylated at S616 by CDK1 complexed with its activator cyclin B to induce mitochondrial fission and permit G2-to-M transition [15]. In addition to increased DRP1 protein expression in PAH PASMCs, DRP1 was found to be hyper-phosphorylated at S616, suggesting that increased DRP1 levels are accompanied by increased activity. Marsboom et al. [20] reported a similar finding and implicated the cell cycle regulator CDK1 and its activator cyclin B as the key drivers of DRP1 hyper-phosphorylation in PAH PASMCs. They showed that inhibiting CDK1 with RO-3306 markedly reduced DRP1 phosphorylation at S616. However, inhibiting other serine/threonine kinases known to phosphorylate DRP1 at S616, such as CaMKII, had no effect on DRP1 phosphorylation in PAH PASMCs [20]. Recently, the pro-proliferative kinase ERK2 has also been shown to phosphorylate DRP1 at S616 and may therefore contribute to the hyper-phosphorylation observed in PAH PASMCs [14]. Indeed, Feng et al. [34] showed that ERK-dependent DRP1 phosphorylation and consequent mitochondrial fission underlie

the pro-proliferative and pro-migratory effects of damage-associated molecular pattern HMGB1 on rat PASMCs. The role of stimulatory DRP1 phosphorylation at S616 in driving vascular remodelling in PAH can be further supported by in vivo studies using Sugen 5416/hypoxia rat models [35], in which the DRP1 gene is edited by 3-component CRISPR to introduce a non-phosphorylatable alanine in place of S616 in the DRP1 protein [36].

Conversely to mitochondrial fission, mitochondrial fusion involves the merging of two mitochondria into one mitochondrion [37]. It requires the end-to-end collision of mitochondria and the fusion of the OMM followed by that of the IMM, culminating in content mixing to distribute matrix components throughout the newly formed mitochondrion [37]. Fusion of the OMM is mediated by the two GTPases MFN1 and MFN2, whereas that of the IMM is carried out by OPA1 [37]. Given the increased mitochondrial fission in PAH PASMCs, it was postulated that the fusion machinery, comprised of these three GTPases, might be downregulated. Marsboom et al. [20] demonstrated a reduction in the mRNA levels of MFN2 but not MFN1 in PAH PASMCs compared to control PASMCs. Contrastingly, this study demonstrated that the protein levels of MFN1 and MFN2 in PAH PASMCs are not significantly different from those in control PASMCs, suggesting that the OMM fusion machinery remains intact in PAH PASMCs. We also show that the protein level of OPA1 in PAH PASMCs was comparable to that in their control counterparts, suggesting that the IMM fusion machinery also remains unaltered and that the excessive mitochondrial fragmentation in PAH PASMCs is a consequence of solely increased fission. It is possible, however, that the post-translational modifications of these proteins, such as ERK-mediated threonine phosphorylation of MFN1 and tyrosine phosphorylation of MFN2, may be altered in PAH [38–40]. This notion has not been tested in this study and warrants further investigation.

Several studies suggest that mitochondrial fission is required for cell cycle progression to mitosis and is increased in many different highly proliferative cells, such as PAH PASMCs [15,20,41]. Indeed, inhibiting DRP1 with either siRNA-mediated knockdown or the small molecule inhibitor Mdivi-1 was found to promote mitochondrial elongation, induce G2/M cell cycle arrest, and inhibit proliferation in PAH PASMCs [20]. Prostacyclin analogues have been shown to inhibit the proliferation of PASMCs by inducing cell cycle arrest at the G1/S checkpoint [28]. This study investigated whether the stable prostacyclin analogue treprostinil attenuates excessive mitochondrial fragmentation in PAH PASMCs. Treatment of PAH PASMCs with treprostinil was found to rapidly decrease the numbers of mitochondrial individuals and networks in PAH PASMCs. Treprostinil also increased the lengths of mitochondrial branches and the number of mitochondrial branches per mitochondrial network. These effects were comparable to those of the DRP1 small-molecule inhibitor Mdivi1. Collectively, these results suggest that, in PAH PASMCs, treprostinil promotes the formation of fewer, larger, highly branched mitochondrial networks that hinder cell cycle progression into the M phase and hence PASMC proliferation.

DRP1 activity is decreased by phosphorylation at S637 [17]. This inhibitory DRP1 phosphorylation is mediated by the cAMP-dependent serine/threonine kinase PKA [17]. Given the pro-fusion effect of treprostinil on mitochondrial dynamics and its previously reported ability to evoke an increase in intracellular cAMP levels in PAH PASMCs [26–28,42], it was suggested that treprostinil might be inhibiting DRP1 activity by stimulating its phosphorylation at S637. Prior to the addition of treprostinil, very little if any DRP1 phosphorylation at S637 was observed in PAH PASMCs, suggesting that DRP1 could be maintained in a dephosphorylated state by calcineurin [16] or the breakdown of constitutively generated cAMP by phosphodiesterases (PDEs), the activity of which is known to be elevated in PAH [43]. Treprostinil rapidly induced DRP1 phosphorylation at S637 in PAH PASMCs without affecting total DRP1 protein levels. However, this DRP1 phosphorylation was transient and only lasted for 6 h, disappearing completely after 24 h. Treprostinil binds to cell-surface prostanoid receptors, which couple to and activate membrane-bound adenylyl cyclase, culminating in cytosolic cAMP generation [26,42]. To trigger the PKA-dependent phosphorylation of DRP1 at S637, cAMP generated near the plasma membrane would have to diffuse to the mitochondria, encountering on its way numerous cAMP-hydrolysing PDE isoforms, such as PDE2, the inhibition of which has been shown to augment PAH PASMC responses to treprostinil [44]. Degradation of treprostinil-induced cAMP could therefore underlie the transiency of its stimulation of DRP1 inhibitory phosphorylation at S637. Treprostinil also inhibited DRP1 phosphorylation at S616. In contrast to the short-lived treprostinil-induced DRP1 phosphorylation at S637, the inhibition of DRP1 phosphorylation at S616 by treprostinil lasted for 24 h and was therefore more sustained. Taken together, these results suggest that treprostinil inhibits DRP1 activity in PAH PASMCs by stimulating its inhibitory phosphorylation at S637 and inhibiting its stimulatory phosphorylation at S616. These results also indicate that the sustained inhibition of DRP1 phosphorylation at S616 by treprostinil is more likely to account for its anti-proliferative effect on PAH PASMCs than the transitory stimulation of DRP1 phosphorylation at S637. Although not investigated in this study, treprostinil may via PKA also promote the phosphorylation of mitochondrial fusion proteins, such as MFN2 at S442 [45].

Treprostinil has been shown to bind with high affinity to the EP_2, DP_1 and IP prostanoid receptors but to inhibit the proliferation of PASMCs from PAH patients predominantly via the EP_2 and to a much lesser degree via the IP receptor [26,27]. Selective receptor antagonists were used to identify the receptors through which treprostinil signals to induce DRP1 phosphorylation at S637 and to inhibit that at S616. Individually, the IP receptor-selective antagonist RO1138452 and the EP_2 receptor-selective antagonist PF04418948 had no effect on treprostinil-induced phosphorylation of DRP1 at S637. When given together, however, the antagonists completely blocked treprostinil-induced DRP1 phosphorylation at S637, suggesting that treprostinil recruits either the IP or EP_2 receptor to stimulate inhibitory DRP1 phosphorylation at S637. Similarly, antagonising the IP and EP_2 receptors individually failed to reverse the treprostinil-mediated inhibition of DRP1 phosphorylation at S616. In combination, the IP and EP_2 receptor antagonists fully reversed the inhibition of DRP1 phosphorylation at S616 that was caused by treprostinil, indicating that treprostinil can activate either receptor to inhibit this stimulatory phosphorylation event. The IP and EP_2 receptors couple via Gs to activate membrane-bound adenylate cyclase and elevate intracellular cAMP, which in turn activates PKA [26,27,31,42]. To determine whether PKA mediates the effect of treprostinil on DRP1 phosphorylation at both serine residues downstream of the IP and EP_2 receptors, the relatively PKA-selective inhibitor H89 was used. Inhibition of PKA blocked treprostinil-induced DRP1 phosphorylation at S637. PKA inhibition also completely reversed the treprostinil-mediated inhibition of DRP1 phosphorylation at S616. The mitochondrial fusogenic effect of treprostinil on PAH PASMCs was associated with a growth suppressive effect that was partially reversed by EP_2 receptor blockade and abolished by combined IP and EP2 receptor antagonism. Taken together, these results support a new pathway for the inhibition of DRP1 activity in PAH PASMCs, in which IP or EP_2 receptor agonism signals via PKA to induce DRP1 phosphorylation at the inhibitory residue S637 and inhibit that at the stimulatory residue S616. PKA-mediated phosphorylation of DRP1 at S637 downstream of IP or EP_2 receptors may also promote efficient mitophagy of dysfunctional mitochondria, which have been proposed to underlie the pathological behaviour of PAH PASMCs [46].

To confirm the roles of the IP and EP_2 receptors in inhibiting DRP1 activity in PAH PASMCs, agonists selective for the IP and EP_2 receptor were used. MRE-269 is the active metabolite of the non-prostanoid IP receptor agonist and PAH drug selexipag and was developed because it was devoid of activity at other prostanoid receptors [47]. Like treprostinil, MRE-269 induced inhibitory DRP1 phosphorylation at S637 and inhibited activating DRP1 phosphorylation at S616 in PAH PASMCs. This was blocked by IP receptor antagonism with RO1138452, confirming the selectivity of MRE-269 for the IP receptor and the ability of

the IP receptor to signal to inhibit DRP1 via the induction of S637 phosphorylation and the inhibition of S616 phosphorylation in PAH PASMCs. This also suggests that, despite the downregulation of the IP receptor in PAH PASMCs [26,27], the number of IP receptors available are sufficient to deliver a signal that promotes DRP1 phosphorylation at S637, while inhibiting phosphorylation at S616. The EP_2 receptor agonist butaprost also induced DRP1 phosphorylation at S637 and inhibited DRP1 phosphorylation at S616. This was blocked by the EP_2 receptor antagonist PF04418948, further supporting the role of EP_2 receptor in inhibiting DRP1 activity through stimulation of inhibitory S637 phosphorylation. Butaprost and MRE-269 also attenuated mitochondrial fission in PAH PASMCs. Butaprost and MRE-269 both similarly decreased the numbers of mitochondrial networks and mitochondrial individuals in PAH PASMCs. They also increased mitochondrial branching and lengthened mitochondrial branches.

5. Conclusion

In summary, this study has uncovered a novel pathway whereby prostacyclin mimetics inhibit DRP1-mediated mitochondrial hyperfragmentation in PAH PASMCs to attenuate their pathological hyperproliferative phenotype. Treprostinil recruits either the IP or EP_2 prostanoid receptor subtypes to activate PKA, most likely via cytosolic cAMP generation, promote the PKA-dependent inhibitory phosphorylation of DRP1 at S637, inhibit stimulatory DRP1 phosphorylation at S616 and reduce proliferation in the overtly proliferative PASMCs derived from PAH patients. The EP_2 receptor agonist butaprost and the IP receptor agonist MRE-269 also inhibited the excessive DRP1-mediated mitochondrial fission in a treprostinil-like fashion. These results suggest that DRP1 may already be targeted in PAH patients on prostacyclin mimetics to inhibit the mitochondrial fragmentation that is associated with PASMC hyper-proliferation and the resultant pulmonary vascular remodelling.

Funding

Jeries Abu-Hanna was funded by the UCL Overseas Research Scholarship. Evangelos Anastasakis was supported by the 2019 Association of Clinical Pathologists Student Research Fund Award. Jan-Willem Taanman obtained funding from the Royal Free Charity (Fund 97). David Abraham obtained funding from Versus Arthritis (formerly Arthritis UK; codes: 2180 and 19427), the Royal Free Charity (Fund 97), Scleroderma and Raynaud's UK and The Rosetrees Trust (code: M96-F1/F2).

CRediT authorship contribution statement

Jeries Abu-Hanna: Conceptualization, Investigation, Formal analysis, Visualization, Writing – original draft. **Evangelos Anastasakis:** Investigation, Formal analysis, Visualization, Writing – original draft. **Jigisha A. Patel:** Resources, Writing – review & editing. **Mohammad Mahmoud Rajab Eddama:** Writing – review & editing. **Christopher P. Denton:** Writing – review & editing. **Jan-Willem Taanman:** Conceptualization, Supervision, Resources, Writing – review & editing. **David Abraham:** Conceptualization, Supervision, Project administration, Funding acquisition, Resources, Writing – review & editing. **Lucie H. Clapp:** Conceptualization, Supervision, Project administration, Resources, Funding acquisition, Writing – review & editing.

Declaration of Competing Interest

The authors declare no conflicts of interest relevant to this study.

Data availability

Data will be made available on request.

Appendix A. Supplementary data

Supplementary data to this article can be found online at https://doi.org/10.1016/j.vph.2023.107194.

References

[1] P.M. Hassoun, Pulmonary arterial hypertension, N. Engl. J. Med. 385 (25) (2021) 2361–2376, https://doi.org/10.1056/NEJMra2000348.
[2] T. Thenappan, M.L. Ormiston, J.J. Ryan, et al., Pulmonary arterial hypertension: pathogenesis and clinical management, BMJ 360 (2018) j5492, https://doi.org/10.1136/bmj.j5492.
[3] R.M. Tuder, J.C. Marecki, A. Richter, et al., Pathology of pulmonary hypertension, Clin. Chest Med. 28 (1) (2007) 23–42, vii, https://doi.org/10.1016/j.ccm.2006.11.010. vii.
[4] N.S.H. Lan, B.D. Massam, S.S. Kulkarni, et al., Pulmonary arterial hypertension: pathophysiology and treatment, Diseases 6 (2) (2018), https://doi.org/10.3390/diseases6020038.
[5] F. Perros, P. Sentenac, D. Boulate, et al., Smooth muscle phenotype in idiopathic pulmonary hypertension: hyper-proliferative but not cancerous, Int. J. Mol. Sci. 20 (14) (2019), https://doi.org/10.3390/ijms20143575.
[6] B. Lechartier, N. Berrebeh, A. Huertas, et al., Phenotypic diversity of vascular smooth muscle cells in pulmonary arterial hypertension: implications for therapy, Chest 161 (1) (2022) 219–231, https://doi.org/10.1016/j.chest.2021.08.040.
[7] S.L. Archer, G. Marsboom, G.H. Kim, et al., Epigenetic attenuation of mitochondrial superoxide dismutase 2 in pulmonary arterial hypertension: a basis for excessive cell proliferation and a new therapeutic target, Circulation 121 (24) (2010) 2661–2671, https://doi.org/10.1161/CIRCULATIONAHA.109.916098.
[8] R. Paulin, E.D. Michelakis, The metabolic theory of pulmonary arterial hypertension, Circ. Res. 115 (1) (2014) 148–164, https://doi.org/10.1161/CIRCRESAHA.115.301130.
[9] S.L. Archer, Pyruvate kinase and Warburg metabolism in pulmonary arterial hypertension: uncoupled glycolysis and the Cancer-like phenotype of pulmonary arterial hypertension, Circulation 136 (25) (2017) 2486–2490, https://doi.org/10.1161/CIRCULATIONAHA.117.031655.
[10] X. Liu, L. Zhang, W. Zhang, Metabolic reprogramming: a novel metabolic model for pulmonary hypertension, Front. Cardiovasc. Med. 9 (2022) 957524, https://doi.org/10.3389/fcvm.2022.957524.
[11] S.L. Archer, Mitochondrial dynamics–mitochondrial fission and fusion in human diseases, N. Engl. J. Med. 369 (23) (2013) 2236–2251, https://doi.org/10.1056/NEJMra1215233.
[12] D.C. Chan, Mitochondrial dynamics and its involvement in disease, Annu. Rev. Pathol. 15 (2020) 235–259, https://doi.org/10.1146/annurev-pathmechdis-012419-032711.
[13] M. Giacomello, A. Pyakurel, C. Glytsou, et al., The cell biology of mitochondrial membrane dynamics, Nat. Rev. Mol. Cell Biol. 21 (4) (2020) 204–224, https://doi.org/10.1038/s41580-020-0210-7.
[14] J.A. Kashatus, A. Nascimento, L.J. Myers, et al., Erk2 phosphorylation of Drp1 promotes mitochondrial fission and MAPK-driven tumor growth, Mol. Cell 57 (3) (2015) 537–551, https://doi.org/10.1016/j.molcel.2015.01.002.
[15] N. Taguchi, N. Ishihara, A. Jofuku, et al., Mitotic phosphorylation of dynamin-related GTPase Drp1 participates in mitochondrial fission, J. Biol. Chem. 282 (15) (2007) 11521–11529, https://doi.org/10.1074/jbc.M607279200.
[16] G.M. Cereghetti, A. Stangherlin, O. Martins de Brito, et al., Dephosphorylation by calcineurin regulates translocation of Drp1 to mitochondria, Proc. Natl. Acad. Sci. U. S. A. 105 (41) (2008) 15803–15808, https://doi.org/10.1073/pnas.0808249105.
[17] C.R. Chang, C. Blackstone, Cyclic AMP-dependent protein kinase phosphorylation of Drp1 regulates its GTPase activity and mitochondrial morphology, J. Biol. Chem. 282 (30) (2007) 21583–21587, https://doi.org/10.1074/jbc.C700083200.
[18] C.R. Chang, C. Blackstone, Drp1 phosphorylation and mitochondrial regulation, EMBO Rep. 8 (12) (2007) 1088–1089, author reply 1089-90, https://doi.org/10.1038/sj.embor.7401118. author reply 1089-90.
[19] J.T. Cribbs, S. Strack, Reversible phosphorylation of Drp1 by cyclic AMP-dependent protein kinase and calcineurin regulates mitochondrial fission and cell death, EMBO Rep. 8 (10) (2007) 939–944, https://doi.org/10.1038/sj.embor.7401062.
[20] G. Marsboom, P.T. Toth, J.J. Ryan, et al., Dynamin-related protein 1-mediated mitochondrial mitotic fission permits hyperproliferation of vascular smooth muscle cells and offers a novel therapeutic target in pulmonary hypertension, Circ. Res. 110 (11) (2012) 1484–1497, https://doi.org/10.1161/CIRCRESAHA.111.263848.
[21] K.H. Chen, A. Dasgupta, J. Lin, et al., Epigenetic dysregulation of the dynamin-related protein 1 binding partners MiD49 and MiD51 increases mitotic mitochondrial fission and promotes pulmonary arterial hypertension: mechanistic and therapeutic implications, Circulation 138 (3) (2018) 287–304, https://doi.org/10.1161/CIRCULATIONAHA.117.031258.
[22] N.F. Ruopp, B.A. Cockrill, Diagnosis and treatment of pulmonary arterial hypertension: a review, JAMA 327 (14) (2022) 1379–1391, https://doi.org/10.1001/jama.2022.4402.
[23] Z.C. Jing, K. Parikh, T. Pulido, et al., Efficacy and safety of oral treprostinil monotherapy for the treatment of pulmonary arterial hypertension: a randomized, controlled trial, Circulation 127 (5) (2013) 624–633, https://doi.org/10.1161/CIRCULATIONAHA.112.124388.

[24] Y. Li, M. Connolly, C. Nagaraj, et al., Peroxisome proliferator-activated receptor-β/δ, the acute signaling factor in prostacyclin-induced pulmonary vasodilation, Am. J. Respir. Cell Mol. Biol. 46 (3) (2012) 372–379, https://doi.org/10.1165/rcmb.2010-0428OC.
[25] L.H. Clapp, R. Gurung, The mechanistic basis of prostacyclin and its stable analogues in pulmonary arterial hypertension: role of membrane versus nuclear receptors, Prostaglandins Other Lipid Mediat. 120 (2015) 56–71, https://doi.org/10.1016/j.prostaglandins.2015.04.007.
[26] E. Falcetti, S.M. Hall, P.G. Phillips, et al., Smooth muscle proliferation and role of the prostacyclin (IP) receptor in idiopathic pulmonary arterial hypertension, Am. J. Respir. Crit. Care Med. 182 (9) (2010) 1161–1170, https://doi.org/10.1164/rccm.201001-0011OC.
[27] J.A. Patel, L. Shen, S.M. Hall, et al., Prostanoid EP_2 receptors are up-regulated in human pulmonary arterial hypertension: a key anti-proliferative target for Treprostinil in smooth muscle cells, Int. J. Mol. Sci. 19 (8) (2018), https://doi.org/10.3390/ijms19082372.
[28] J. Wharton, N. Davie, P.D. Upton, et al., Prostacyclin analogues differentially inhibit growth of distal and proximal human pulmonary artery smooth muscle cells, Circulation 102 (25) (2000) 3130–3136, https://doi.org/10.1161/01.cir.102.25.3130.
[29] J. Yang, X. Li, R.S. Al-Lamki, et al., Smad-dependent and smad-independent induction of id1 by prostacyclin analogues inhibits proliferation of pulmonary artery smooth muscle cells in vitro and in vivo, Circ. Res. 107 (2) (2010) 252–262, https://doi.org/10.1161/CIRCRESAHA.109.209940.
[30] J. Gatfield, K. Menyhart, D. Wanner, et al., Selexipag active metabolite ACT-333679 displays strong Anticontractile and Antiremodeling effects but low, J. Pharmacol. Exp. Ther. 362 (1) (2017) 186–199, https://doi.org/10.1124/jpet.116.239665.
[31] B.J. Whittle, A.M. Silverstein, D.M. Mottola, et al., Binding and activity of the prostacyclin receptor (IP) agonists, treprostinil and iloprost, at human prostanoid receptors: treprostinil is a potent DP1 and EP2 agonist, Biochem. Pharmacol. 84 (1) (2012) 68–75, https://doi.org/10.1016/j.bcp.2012.03.012.
[32] A.J. Valente, L.A. Maddalena, E.L. Robb, et al., A simple ImageJ macro tool for analyzing mitochondrial network morphology in mammalian cell culture, Acta Histochem. 119 (3) (2017) 315–326, https://doi.org/10.1016/j.acthis.2017.03.001.
[33] L.M. Westrate, A.D. Sayfie, D.M. Burgenske, et al., Persistent mitochondrial hyperfusion promotes G2/M accumulation and caspase-dependent cell death, PLoS One 9 (3) (2014), e91911, https://doi.org/10.1371/journal.pone.0091911.
[34] W. Feng, J. Wang, X. Yan, et al., ERK/Drp1-dependent mitochondrial fission contributes to HMGB1-induced autophagy in pulmonary arterial hypertension, Cell Prolif. 54 (6) (2021), e13048, https://doi.org/10.1111/cpr.13048.
[35] S.H. Vitali, G. Hansmann, C. Rose, et al., The Sugen 5416/hypoxia mouse model of pulmonary hypertension revisited: long-term follow-up, Pulm. Circ. 4 (4) (2014) 619–629, https://doi.org/10.1086/678508.
[36] J.M. Miano, Q.M. Zhu, C.J. Lowenstein, A CRISPR path to engineering new genetic mouse models for cardiovascular research, Arterioscler. Thromb. Vasc. Biol. 36 (6) (2016) 1058–1075, https://doi.org/10.1161/ATVBAHA.116.304790.
[37] I. Scott, R.J. Youle, Mitochondrial fission and fusion, Essays Biochem. 47 (2010) 85–98, https://doi.org/10.1042/bse0470085.
[38] A. Dasgupta, K.H. Chen, P.D.A. Lima, et al., PINK1-induced phosphorylation of mitofusin 2 at serine 442 causes its proteasomal degradation and promotes cell proliferation in lung cancer and pulmonary arterial hypertension, FASEB J. 35 (8) (2021), e21771, https://doi.org/10.1096/fj.202100361R.
[39] A. Pyakurel, C. Savoia, D. Hess, et al., Extracellular regulated kinase phosphorylates mitofusin 1 to control mitochondrial morphology and apoptosis, Mol. Cell 58 (2) (2015) 244–254, https://doi.org/10.1016/j.molcel.2015.02.021.
[40] P. Zhang, K. Ford, J.H. Sung, et al., Tyrosine phosphorylation of mitofusin 2 regulates endoplasmic reticulum-mitochondria tethering, bioRxiv (2022), https://doi.org/10.1101/2022.02.21.481295.
[41] B. Spurlock, D. Parker, M.K. Basu, et al., Fine-tuned repression of Drp1-driven mitochondrial fission primes a 'stem/progenitor-like state' to support neoplastic transformation, Elife 10 (2021), https://doi.org/10.7554/eLife.68394.
[42] L.H. Clapp, P. Finney, S. Turcato, et al., Differential effects of stable prostacyclin analogs on smooth muscle proliferation and cyclic AMP generation in human pulmonary artery, Am. J. Respir. Cell Mol. Biol. 26 (2) (2002) 194–201, https://doi.org/10.1165/ajrcmb.26.2.4695.
[43] R.T. Schermuly, S.S. Pullamsetti, G. Kwapiszewska, et al., Phosphodiesterase 1 upregulation in pulmonary arterial hypertension: target for reverse-remodeling therapy, Circulation 115 (17) (2007) 2331–2339, https://doi.org/10.1161/CIRCULATIONAHA.106.676809.
[44] K.J. Bubb, S.L. Trinder, R.S. Baliga, et al., Inhibition of phosphodiesterase 2 augments cGMP and cAMP signaling to ameliorate pulmonary hypertension, Circulation 130 (6) (2014) 496–507, https://doi.org/10.1161/CIRCULATIONAHA.114.009751.
[45] W. Zhou, K.H. Chen, W. Cao, et al., Mutation of the protein kinase a phosphorylation site influences the anti-proliferative activity of mitofusin 2, Atherosclerosis 211 (1) (2010) 216–223, https://doi.org/10.1016/j.atherosclerosis.2010.02.012.
[46] H.J. Ko, C.Y. Tsai, S.J. Chiou, et al., The phosphorylation status of Drp1-Ser637 by PKA in mitochondrial fission modulates Mitophagy via PINK1/Parkin to exert multipolar spindles assembly during mitosis, Biomolecules 11 (3) (2021), https://doi.org/10.3390/biom11030424.
[47] G. Simonneau, A. Torbicki, M.M. Hoeper, et al., Selexipag: an oral, selective prostacyclin receptor agonist for the treatment of pulmonary arterial hypertension, Eur. Respir. J. 40 (4) (2012) 874–880, https://doi.org/10.1183/09031936.00137511.